polymers

MDPI

Review

Functional Polyimide/Polyhedral Oligomeric Silsesquioxane Nanocomposites

Mohamed Gamal Mohamed [1,2] and Shiao Wei Kuo [1,3,*]

[1] Department of Materials and Optoelectronic Science, Center of Crystal Research, National Sun Yat-Sen University, Kaohsiung 80424, Taiwan; mgamal.eldin12@yahoo.com
[2] Chemistry Department, Faculty of Science, Assiut University, Assiut 71516, Egypt
[3] Department of Medicinal and Applied Chemistry, Kaohsiung Medical University, Kaohsiung 807, Taiwan
* Correspondence: kuosw@faculty.nsysu.edu.tw; Tel.: +886-7-525-4099

Received: 11 December 2018; Accepted: 23 December 2018; Published: 25 December 2018

Abstract: The preparation of hybrid nanocomposite materials derived from polyhedral oligomeric silsesquioxane (POSS) nanoparticles and polyimide (PI) has recently attracted much attention from both academia and industry, because such materials can display low water absorption, high thermal stability, good mechanical characteristics, low dielectric constant, flame retardance, chemical resistance, thermo-redox stability, surface hydrophobicity, and excellent electrical properties. Herein, we discussed the various methods that have been used to insert POSS nanoparticles into PI matrices, through covalent chemical bonding and physical blending, as well as the influence of the POSS units on the physical properties of the PIs.

Keywords: polyhedral oligomeric silsesquioxane (POSS); double-decker-shaped silsesquioxane (DDSQ); polyimide; thermal stability; dielectric constant

1. Introduction

Polyhedral oligomeric silsesquioxanes (POSS) form a class of nanostructured materials having diameters on the order of 1–3 nm; they can be considered as the smallest silica nanoparticles (NPs) [1–4]. Polyhedral oligomeric silsesquioxanes (POSS) moieties have the empirical formula $(RSiO_{1.5})_n$, where R may be an organic functional group (e.g., alkyl, alkylene, epoxide unit, acrylate, hydroxyl) or a hydrogen atom, controlled porosity and nanometer sized structure; the structures of POSS NPs can be divided into partial cage, ladder, and random structures [5–9]. The properties of POSS-containing polymers can improve (e.g., decreased flammability, viscosity, and heat discharge, and increased rigidity, strength, and modulus) via the degree of dispersion of the POSS NPs into the polymer matrix [10–26]. Two general approaches have been used to incorporate POSS units into polymer matrices: (i) physical blending [27–30] and (ii) covalent attachment [29–35]. In the physical blending approach, the POSS NPs are blended (through melt-mixing or solvent-casting) with the polymers without forming covalent bonds; the success of this approach depends on the compatibility of the POSS NPs with the polymers [36–38]. In the covalent approach, the POSS NPs are attached to the polymer chain through covalent bonds. Although many types of POSS NP architectures (non-functional, mono-functional, bifunctional, and multi-functional) have been incorporated into polymer matrices (Figure 1), the preparation of polymer/POSS nanocomposites remains challenging because it can be expensive to perform on large scales, can require long equilibrium times, and can result in aggregation of the POSS NPs [39–43].

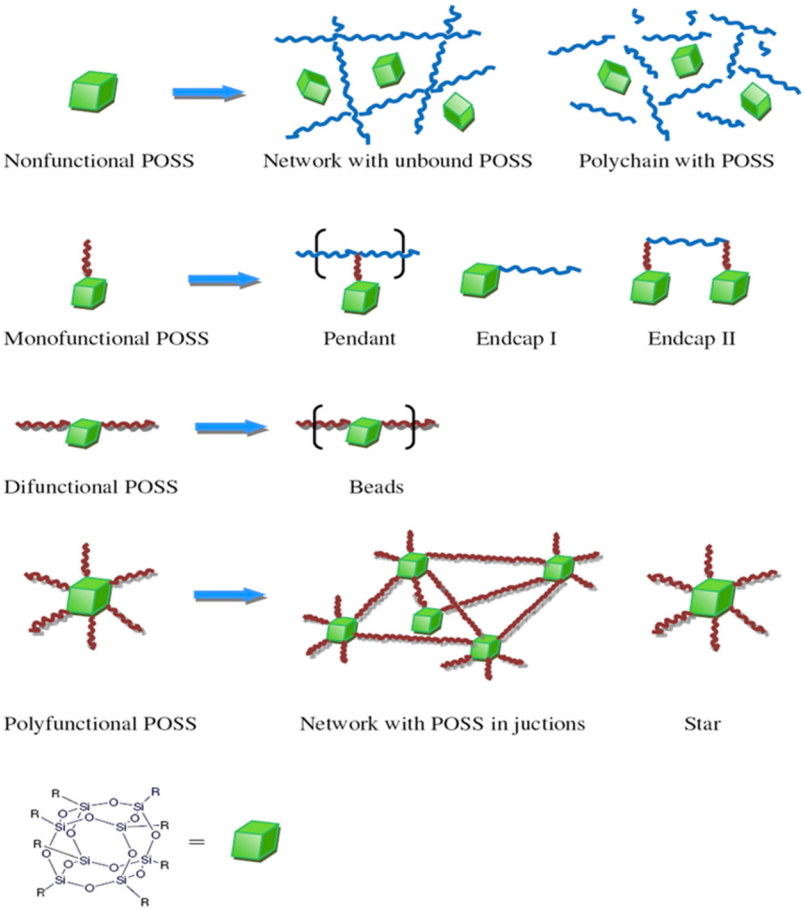

Figure 1. Schematic representation of possible architectures for incorporation of polyhedral oligomeric silsesquioxanes (POSS) nanoparticles (NPs) into polymer matrices [2]. Reproduced with permission from Elsevier.

Polyimide (PI) is an important high-performance material because of its outstanding thermo-oxidative stability, chemical resistance, and mechanical and electrical stability [44–46]. Aromatic polyimides have been applied as insulating materials in many areas, including aerospace and microelectronics [47–61]. Aromatic PIs are polymers featuring stiff aromatic backbones; they are synthesized in two steps: condensation polymerization of an aliphatic or aromatic dianhydride acid and a diamine under ambient conditions in a dipolar aprotic solvent [e.g., *N*,*N*-dimethylacetamide (DMAc), *N*-methylpyrrolidinone (NMP), dimethylsulfoxide (DMSO)] to afford a corresponding poly(amic acid) (PAA), and subsequent ring closure [62–65]. Most aromatic PIs are insoluble and infusible because of their heteroaromatic structures and planar aromatic units. The thermal and mechanical properties of PIs can be enhanced, and their dielectric constants and linear coefficients of thermal expansion decreased, after the incorporation of various inorganic materials (e.g., silica NPs and ceramics) [65–70].

In this Review, we focused on the various methods that have been used to prepare PI/POSS hybrid nanocomposites based on Figure 1, including the blending of non-functional POSS NPs with PIs, the covalent linking of mono-functional POSS NPs with PIs at the chain end or side chain, the covalent incorporation of bifunctional POSS NPs into the PI main chain, and the formation of thermally crosslinked PIs with multi-functional POSS NPs. Additionally, we discussed the physical properties of the resulting PI/POSS nanocomposites, including their dielectric constants and dynamic mechanical, thermal, electrical, and surface properties.

2. PI/POSS Nanocomposites

2.1. Non-Functional POSS NPs Blended with PIs

Chang et al. prepared PI/POSS nanocomposites exhibiting good thermal properties and low dielectric constants through the blending of fluorinated POSS precursors with PI [71]. The fluorinated POSS precursors was prepared by reacting octakis(dimethylsiloxyhexafluoropropyl) silsesquioxane (OF) with allyl 1,1,2,3,3,3-hexafluoropropyl ether (AHFPE) to form OF-POSS NPs, and with allyl propyl ether (APE) to form octakis(propyl ether) silsesquioxane (OP-POSS) NPs, using platinum 1,3-divinyl-1,1,3,3-tetramethyldisiloxane [Pt(dvs)] as the catalyst. Morphological studies revealed the possible occurrence of phase separation in these two PAA/OP and PAA/OF systems after a process of thermal imidization and solvent removal (Figure 2). Based on dynamic mechanical analysis (DMA), the glass transition temperature (T_g) of the PI (371 °C) increased after introduction 10 wt % of the OF-POSS NPs. In contrast, after the incorporation of 15 wt % of the OP-POSS NPs, the values of T_g of the PI (359 °C) decreased relative to that of the corresponding pure PI (366 °C), due to the bulky and rigid POSS units coming into close contact with the polymer chain matrix and increasing the free volume around them [72,73].

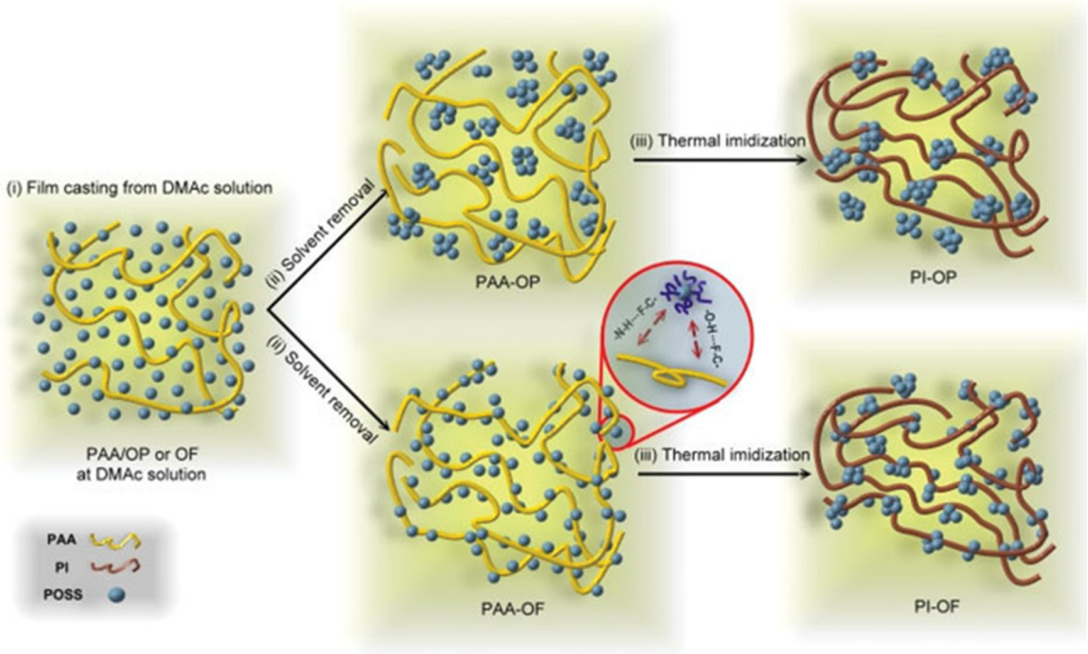

Figure 2. Cartoon representation of the deformation processes of Polyimide (PI)/octakis(dimethylsiloxyhexafluoropropyl) silsesquioxane (OF)-POSS and (OP)-POSS NPs during imidization [71]. Reproduced with permission from Wiley.

Liao et al. [74] prepared octa(aminophenyl)silsesquioxane (OAPS)-functionalized graphene oxide (GO)–reinforced PI nanocomposite films (Figure 3). The tensile strength of the OAPS-GO/PI composite increased 11.2-fold after adding 3 wt % OAPS-GO (Figure 4(a)). In addition, the dielectric constant of the OAPS-GO/PI composite film decreased upon increasing the concentration of OAPS-GO (Figure 4b). Furthermore, we have prepared nanoporous PI films of low dielectric constant (k = 2.25) through blending PI with a star poly(ethylene oxide) PEO-POSS hybrid as a template and then removing the PEO segments through oxidative thermolysis to produce voids inside the polymer matrix (pore sizes: 10–40 nm) [75]. Figure 5 displays the storage moduli and values of tan δ for the pure PI and the porous PI templated by the star PEO-POSS NPs. Through DMA, the pure PI displayed a single value of T_g of 370 °C, while the porous PI exhibited two T_g at 360 and 385 °C. The lower value of T_g corresponded to that typically observed for micro-phase separation from the porous PI, suggesting that the storage

modulus decreased as a result of its foam structure. These foam structures would have collapsed, such that the corresponding porous structures would no longer exist, at higher temperatures, with the residual silica from the star PEO-POSS after thermal calcination enhancing the value of T_g (385 °C) of the porous PI. More importantly, the dielectric constant decreased significantly, from 3.25 to 2.25, for this porous PI matrix.

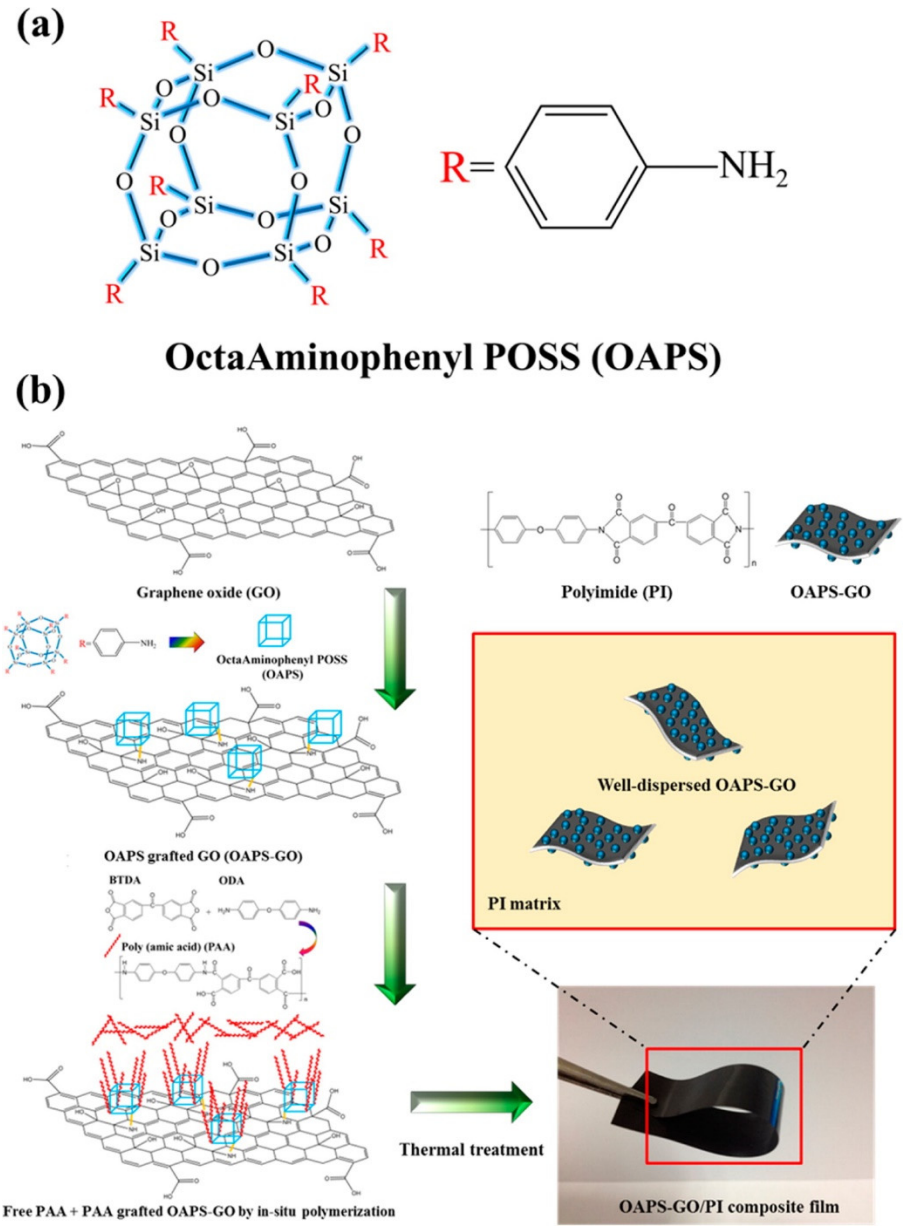

Figure 3. (**a**) Chemical structure of octa(aminophenyl)silsesquioxane (OAPS). (**b**) Schematic representation of the preparation of OAPS-graphene oxide (GO)/PI hybrid nanocomposites [74]. Reproduced with permission from the American Chemical Society.

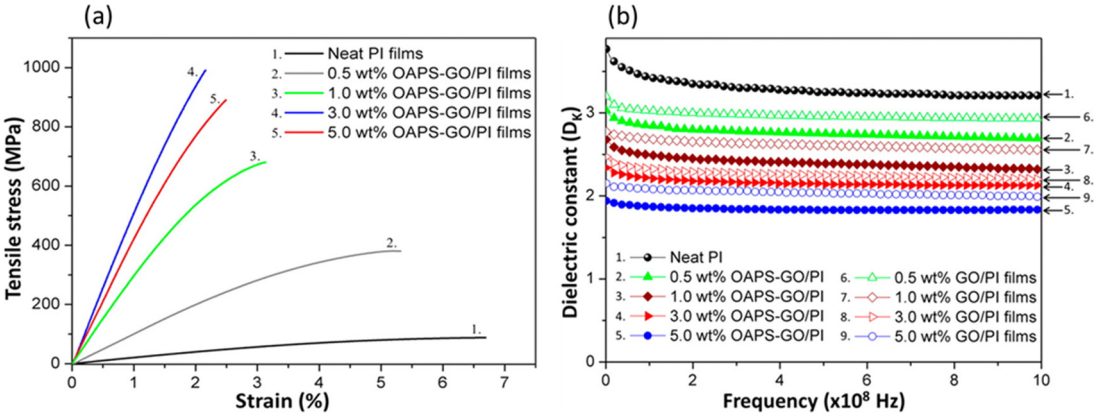

Figure 4. (**a**) Stress–strain curves of neat PI films and OAPS-GO/PI films with different contents of various amounts of OAPS-GO. (**b**) Profile dielectric constants of neat PI films, GO/PI films, and OAPS-GO/PI films [74]. Reproduced with permission from the American Chemical Society.

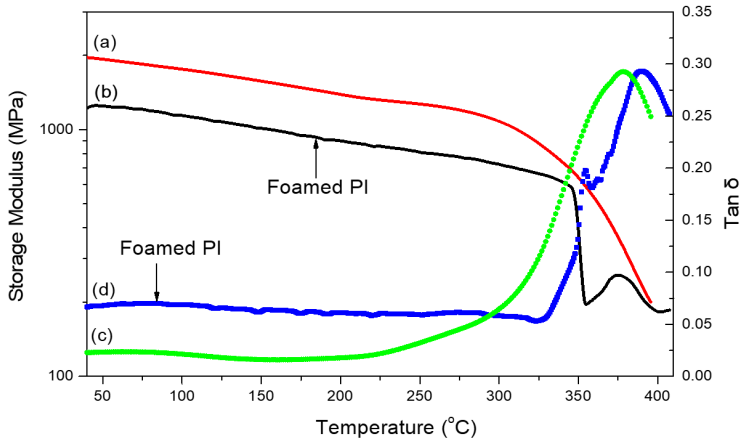

Figure 5. Dynamic mechanical analysis (DMA) curves for (**a**,**c**) pure PI and (**b**,**d**) porous PI (obtained from 10 wt % PEO-POSS), recorded at a heating rate of 2 °C/min [75]. Reproduced with permission from Elsevier.

2.2. *Mono-Functional POSS NPs with PIs*

2.2.1. PIs Containing POSS NPs at Polymer Chain End

Wei et al. [76] prepared nanoporous PI/POSS nanocomposites through a multistep process (Figure 6). First, pyromellitic dianhydride (PMDA) reacted with 4,4′-oxydianiline (ODA) in DMAc under a N_2 atmosphere at room temperature to afford PAA. Then, POSS-NH_2 reacted with PAA in DMAc to obtain PAA/POSS nanocomposites. The PI linked through its chain ends to POSS NPs was obtained after thermal imidization of the PAA/POSS nanocomposites at 300 °C. The dielectric constant of the resultant polyimide POSS nanocomposites decreased from 3.40 for the neat PI to 3.09 after adding 2.5 mol % of POSS units; this behavior was attributed to the phase-separated system and the uniformly porous structure (nanometer-scale) of the POSS molecules. In addition, the resultant PI linked through its chain ends to the POSS NPs formed lamellae or cylinders that were in the range of 60–70 nm long and 5 nm wide (through transmission electron microscope (TEM) image).

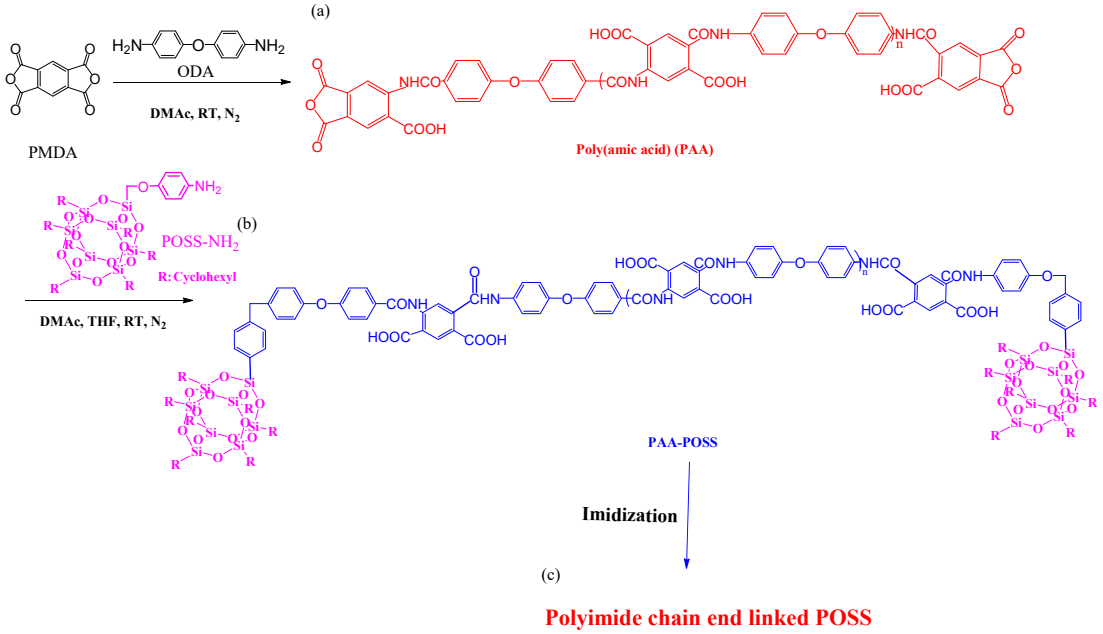

Figure 6. Preparation of (**a**) poly(amic acid) (PAA); (**b**) PAA/POSS nanocomposites; and (**c**) PI linked through its chain ends to POSS [76]. Reproduced with permission from the American Chemical Society.

Zhao et al. [77] synthesized a series of fluorinated PI/POSS hybrid materials through a simple route from 2,2′-bis(trifluoromethyl)benzidine, 4,4′-oxydiphthalic dianhydride, and a monofunctional POSS in m-cresol and isoquinoline as solvents (Figure 7). These hybrid polymers possessed low dielectric constants (in the range 2.47–2.92), high thermal stability, film formation ability, excellent solubility, and good hydrophobic and mechanical properties.

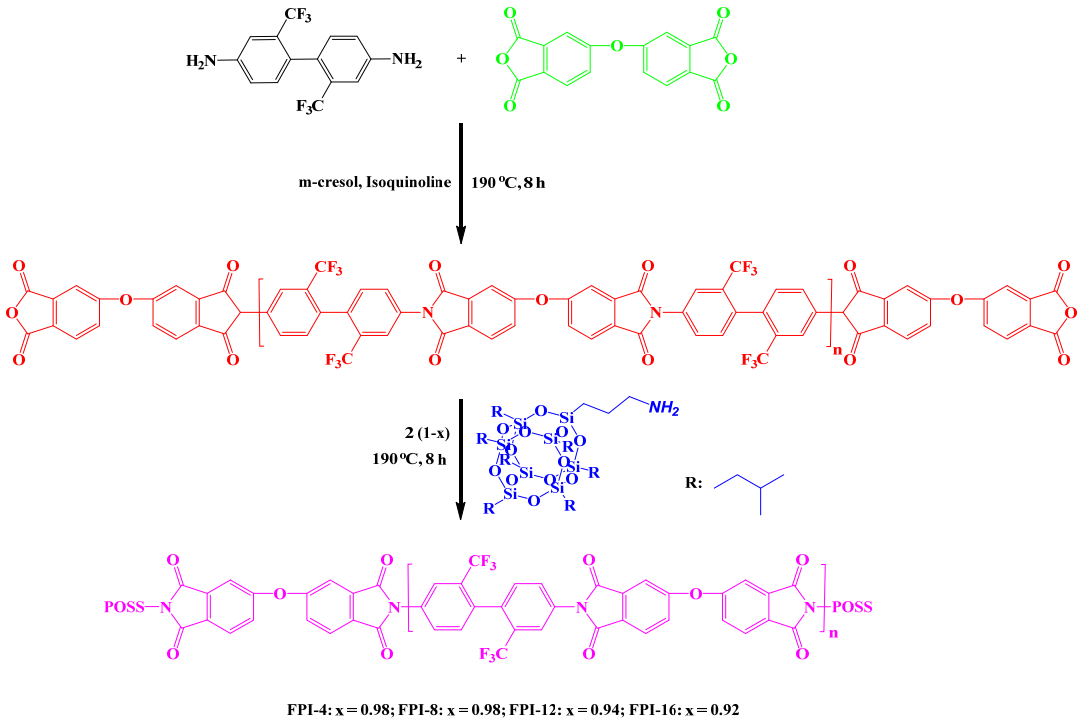

Figure 7. Synthesis of fluorinated PI/POSS hybrid nanocomposites [77]. Reproduced with permission from Springer.

2.2.2. PIs presenting POSS NPs Grafted to the Side Chains

Wei et al. [78] prepared PI-tethered POSS hybrid materials through copolymerization of a POSS-diamine, ODA, with PMDA (Figure 8). When the POSS content was 16 mol %, this PI/POSS composite displayed the large-scale self-assembled layer-by-layer structure of POSS. This layer-by-layer structure of POSS possessed (as elucidated by TEM observations) a layer length of greater than 100 nm and a layer spacing of 2–4 nm. Chen et al. [79] prepared hybrid film materials having tunable dielectric constants, lower than that of the neat PI, through thermally initiated free-radical graft polymerization of methacrylcyclopentyl-POSS (MA-POSS) with ozone-pretreated poly[*N*,*N*-(1,4-phenylene)-3,3′,4,4′-benzophenonetetracarboxylic amic acid] and subsequent thermal imidization to afford PI-*g*-PMA-POSS nanocomposite films. Nuclear magnetic resonance (NMR) spectroscopy, X-ray diffraction (XRD), and thermogravimetric analysis (TGA) confirmed the chemical composition and structure of these PI-*g*-PMA-POSS nanocomposite films.

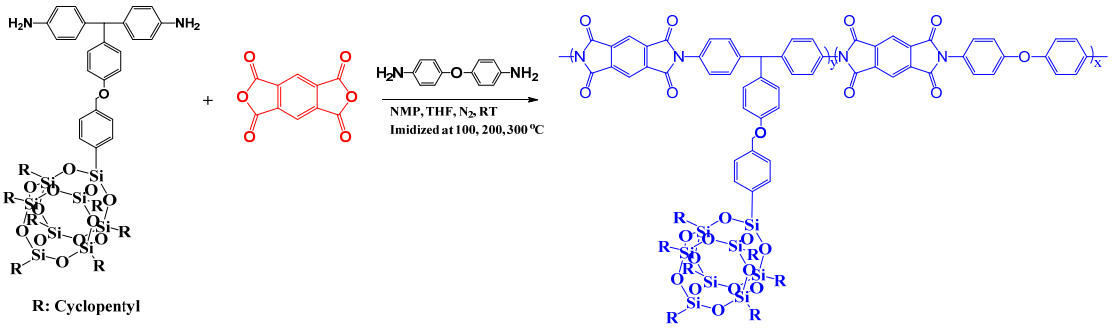

Figure 8. Schematic representation of side chain-tethered PI/POSS nanocomposites [78]. Reproduced with permission from the American Chemical Society.

2.3. Bifunctional POSS NPs Incorporated within the Main Chain of PIs

Kakimoto et al. [80] synthesized various semi-aromatic PIs containing double-decker-shaped silsesquioxane (DDSQ) in the main chain (POSS-PIs) through the reactions of DDSQ-diamine, which was prepared through hydrosilylation of DDSQ with cis-5-norbornene-endo-2,3-dicarboxylic anhydride and a subsequent reaction with ODA. The DDSQ-NH_2 reacted with various aromatic tetracarboxylic dianhydrides to obtain POSS-PIs nanocomposites (Figure 9). The POSS-PIs had low water absorption, low dielectric constants, and good thermal stabilities. In addition, the polymer hybrid materials films had good mechanical properties, with an elongation at breakage of 2.9–6.0%. Zheng et al. [81] synthesized a PI containing a tetrafunctional POSS through thermal imidization of 5,11,14,17-tetranilino DDSQ with 4,4′-diaminophenylether (ODA) and 3,3′,4,4′-benzo phenonetetracarboxylic dianhydride (DTDA) in DMAc, affording organic/inorganic PI nanocomposites incorporating variable contents of POSS units. Based on TGA and surface contact angle measurements (Figure 10a,b), these nanocomposite materials exhibited greater thermal stability and surface hydrophobicity, relative to those of the unmodified PI, upon increasing the POSS content. TEM imaging revealed (Figure 11) that the POSS molecules self-assembled into spherical microdomains having diameters in the range from 40 to 80 nm.

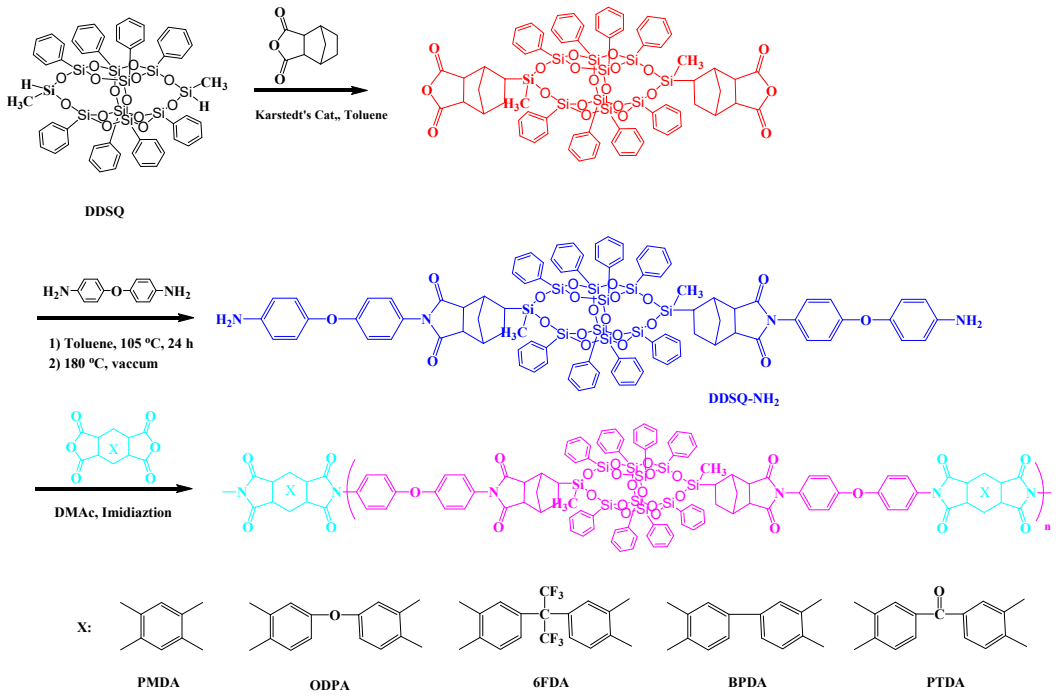

Figure 9. Preparation of semi-aromatic PIs containing a double-decker-shaped silsesquioxane (DDSQ) in the main chain [80]. Reproduced with permission from the American Chemical Society.

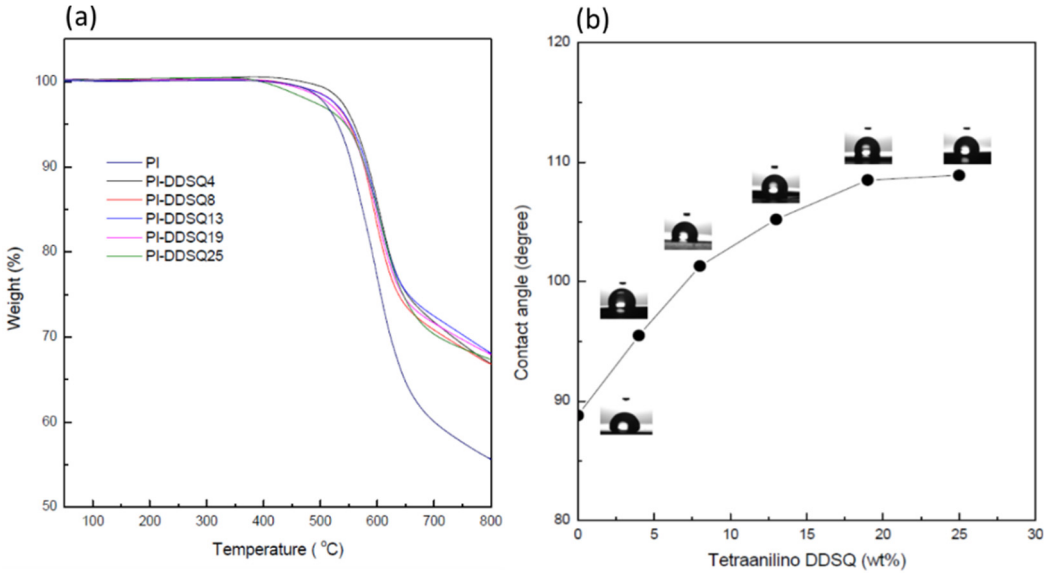

Figure 10. (**a**) Thermogravimetric analysis (TGA) thermogram and (**b**) water contact angles of PIs containing various contents of 5,11,14,17-tetranilino DDSQ [81]. Reproduced with permission from Wiley.

Zheng et al. [82] reported a facile synthetic method for the preparation of organic/inorganic PI with DDSQ in the main chain (Figure 12). First, a DDSQ-diamine was synthesized through a Heck reaction of 3,13-divinyloctaphenyl double-decker silsesquioxane (3,13-divinyl DDSQ) with 4-bromoaniline in the presence of a palladium catalyst; next, thermal imidization of the 3,13-dianilino DDSQ with ODA and 3,3′,4,4′-benzophenonetetracarboxylic in DMAc afforded PI/DDSQ nanocomposites.

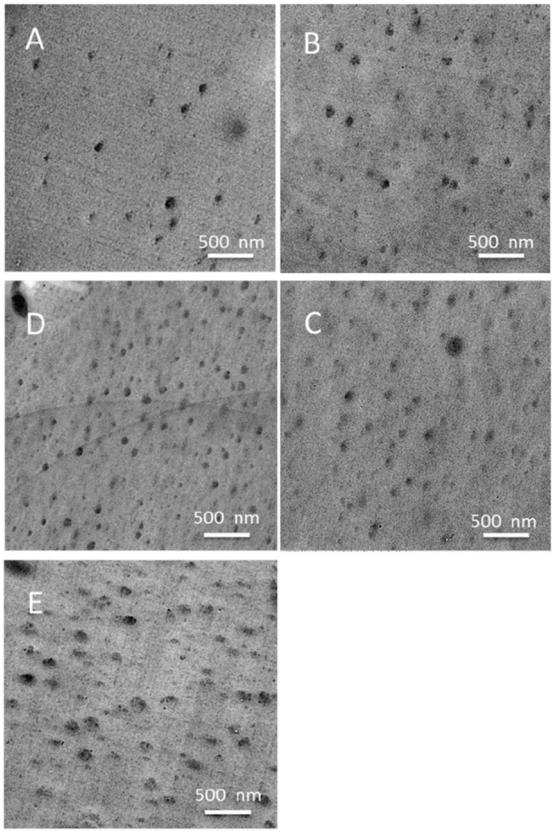

Figure 11. TEM micrographs of the synthesis of PIs containing various contents of 5,11,14,17 tetranilino DDSQ [81]. Reproduced with permission from Wiley.

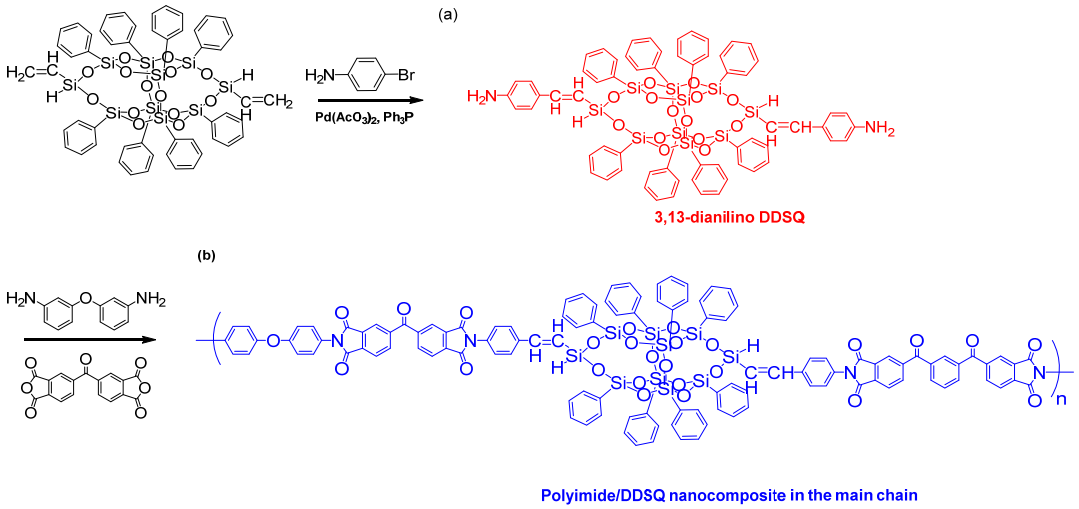

Figure 12. Preparation of organic/inorganic PIs with DDSQ in the main chain [82]. Reproduced with permission from the Royal Society of Chemistry.

According to the dielectric analysis, the dielectric constant of the PI/DDSQ nanocomposites decreased upon incorporating larger amounts of the DDSQ into the main chain (Figure 13). Furthermore, the thermal stability and surface hydrophobicity of the organic/inorganic nanocomposites were enhanced after the inclusion of the DDSQ in the main chain.

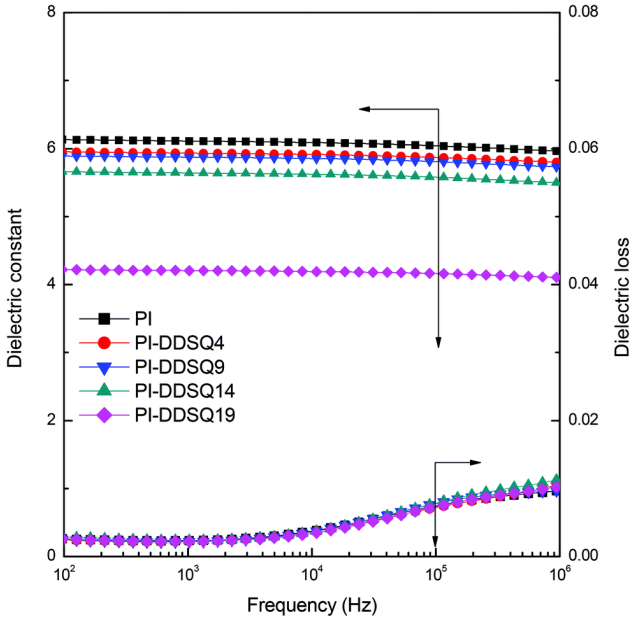

Figure 13. Plots of dielectric constant of organic/inorganic PIs with DDSQ in the main chain [82]. Reproduced with permission from the Royal Society of Chemistry.

2.4. Thermally Crosslinked PIs Incorporating Multi-Functional POSS NPs

We have prepared well-defined PI hybrid materials containing POSS NPs through the copolymerization of octakis(glycidyldimethylsiloxy)octasilsesquioxane (OG-POSS), 4,4′-carbonyldiphthalic anhydride (BTDA), and 4,4′-oxydianiline diamine (ODA) (Figure 14) [83]. The PI-POSS hybrid materials had low dielectric constants and thermal expansion coefficients that decreased from 66.23 to 63.28 to 58.25 ppm/°C when the POSS content increased from 0 to 10 wt %, presumably because of the increase in free volume caused by the presence of the POSS-tethered network.

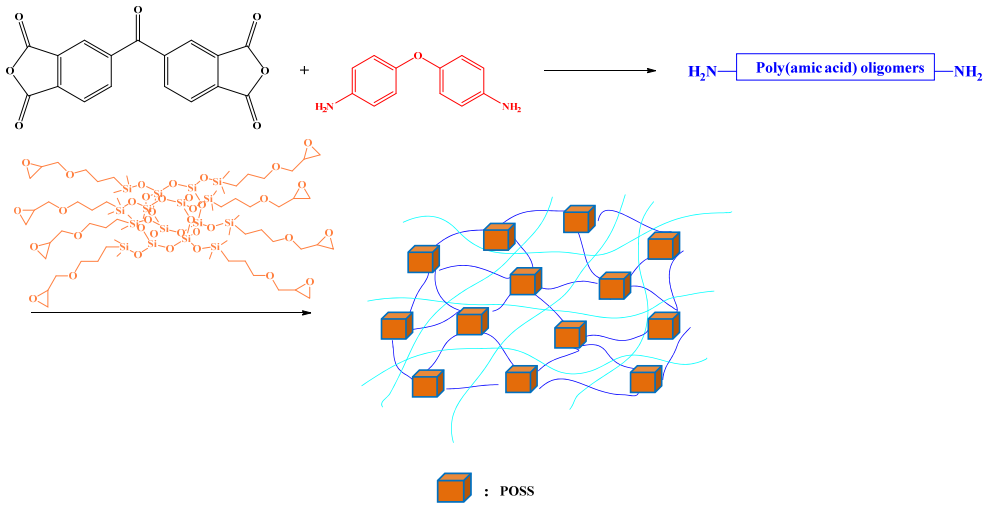

Figure 14. Preparation of OG-POSS cross-linked PIs [83]. Reproduced with permission from Elsevier.

Li et al. prepared a series of octa(aminophenyl)silsesquioxane (OAPS) covalently cross-linked sulfonated PIs (SPIs) (Figure 15) [84]. These OAPS cross-linked PI membranes possessed greater chemical and thermal stability, higher strength, and excellent solution processability when compared with those of the linear sulfonated PI membrane. Moreover, when the OAPS content was 0.4 mol %, the proton conductivity of the cross-linked SPI membrane reached its highest value (0.111 S/cm).

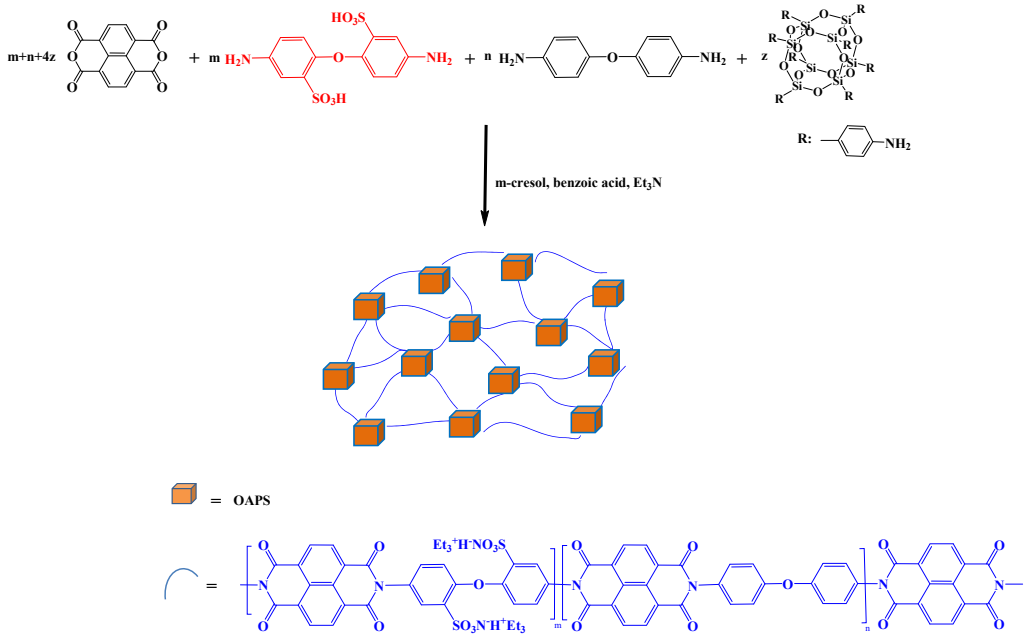

Figure 15. Preparation of POSS cross-linked cross-linked sulfonated PIs (SPIs) [84]. Reproduced with permission from Elsevier.

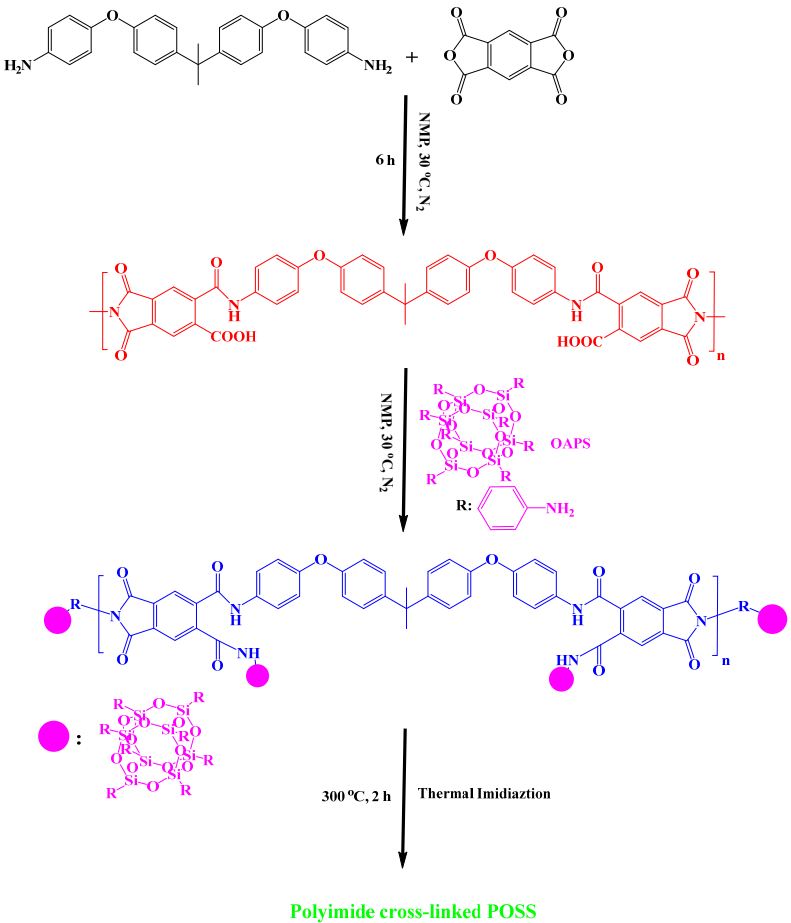

Figure 16. Schematic representation of PI cross-linked POSS [85]. Reproduced with permission from Elsevier.

Alagar et al. synthesized PI/POSS hybrid) materials through a two-step method (Figure 16) [85]. First, the formation of PAA from bisphenol-A ether diamine (BAED) and PMDA in NMP under N_2 at 30 °C, and its blending with various percentages of OAPS; subsequently, thermal imidization of the PAA/OAPS nanocomposites at 300 °C to obtain the POSS-PI nanocomposites. Thermal studies revealed that the glass transition temperature, char yield, thermal stability, and flame-retardant properties of the POSS-PI hybrid nanocomposite were all greater than those of the pristine PI. Adıguzel et al. [86] prepared star polyimides containing polyhedralsilsesquioxane as the core through in situ thermal curing of PAA with octa(aminopolyhedralsilsesquioxane) (Figure 17). The POSS-PI star nanocomposites exhibited unique characteristics including low water absorption, low dielectric constant, and good mechanical and thermal properties arising from the insertion of the rigid POSS units in the PI backbone.

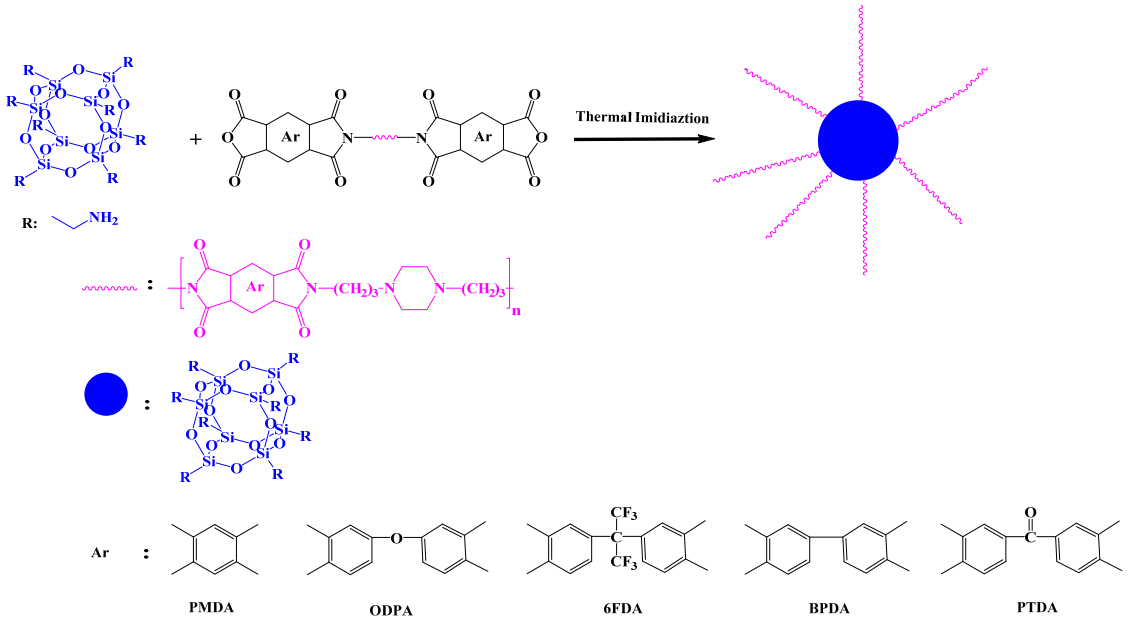

Figure 17. Preparation of star POSS/PI hybrid materials [86]. Reproduced with permission from Elsevier.

3. Conclusions

In this Review, we discussed various preparation types of PIs containing POSS NPs that displayed attractive characteristics, including low dielectric constants, low water absorption, and methanol permeability; excellent mechanical and electrical properties; and high thermal stability, surface hydrophobicity, flame retardance, chemical resistance, proton conductivity, and thermo-redox stability compared with those of their pristine PI precursors. The insertion of these POSS units into the PI precursors has been performed through either physical blending or covalent bonding. The preparation of organic/inorganic hybrid materials containing POSS and PI remains an interesting topic in academic and industrial science because of their potential applications in fuel cells and gas separation membranes, as insulator materials in microelectronics, and in the aerospace industry.

Author Contributions: M.G.M. and S.W.K. both contributed to the literature review and to the writing of this paper.

Conflicts of Interest: The authors declare no conflict of interest.

References

1. Shea, K.J.; Loy, D.A. Bridged polysilsesquioxanes. Molecular-engineered hybrid Organic-inorganic materials. *Chem. Mater.* **2001**, *13*, 3306–3319. [CrossRef]
2. Kuo, S.W.; Chang, F.C. POSS related polymer nanocomposites. *Prog. Polym. Sci.* **2011**, *36*, 1649–1696. [CrossRef]
3. Cordes, D.B.; Lickiss, P.D.; Rataboul, F. Recent developments in the chemistry of cubic polyhedral oligosilsesquioxanes. *Chem. Rev.* **2010**, *110*, 2081–2173. [CrossRef] [PubMed]
4. Wu, J.; Mather, P.T. POSS polymers: Physical properties and biomaterials applications. *Polym. Rev.* **2009**, *49*, 25–63. [CrossRef]
5. Li, Z.; Kong, J.; Wang, F.; He, C. Polyhedral oligomeric silsesquioxanes (POSSs): An important building block for organic optoelectronic materials. *J. Mater. Chem. C* **2017**, *5*, 5283–5298. [CrossRef]
6. Li, Z.; Tan, B.H.; Jin, G.; Li, K.; He, C. Design of polyhedral oligomeric silsesquioxane (POSS) based thermo-responsive amphiphilic hybrid copolymers for thermally denatured protein protection applications. *Polym. Chem.* **2014**, *5*, 6740–6753. [CrossRef]
7. Blanco, I.; Bottino, F.A.; Bottino, P. Influence of symmetry/asymmetry of the NPs structure on the thermal stability of polyhedral oligomeric silsesquioxane/polystyrene nanocomposites. *Polym. Compos.* **2012**, *33*, 1903–1910. [CrossRef]
8. Moore, B.M.; Ramirez, S.M.; Yandek, G.R.; Haddad, T.S.; Mabry, J.M. Asymmetric aryl polyhedral oligomeric silsesquioxanes (ArPOSS) with enhanced solubility. *J. Organomet. Chem.* **2011**, *696*, 2676–2680. [CrossRef]
9. Kuo, S.W. Building Blocks Precisely from Polyhedral Oligomeric Silsesquioxane Nanoparticles. *ACS Cent. Sci.* **2016**, *2*, 62–64. [CrossRef]
10. Mohamed, M.G.; Jheng, Y.R.; Yeh, S.L.; Chen, T.; Kuo, S.W. Unusual Emission of Polystyrene-Based Alternating Copolymers Incorporating Aminobutyl Maleimide Fluorophore-Containing Polyhedral Oligomeric Silsesquioxane NPs. *Polymers* **2017**, *9*, 103. [CrossRef]
11. Zhang, W.; Camino, G.; Yang, R. Polymer/polyhedral oligomeric silsesquioxane (POSS) nanocomposites: An overview of fire retardance. *Prog. Polym. Sci.* **2017**, *67*, 77–125. [CrossRef]
12. Zhou, Z.; Cui, L.; Zhang, Y.; Zhang, Y.; Yin, N. Preparation and properties of POSS grafted polypropylene by reactive blending. *Eur. Polym. J.* **2008**, *44*, 3057–3066. [CrossRef]
13. Gnanasekaran, D.; Madhaven, K.; Reddy, B. Developments of polyhedral oligomeric silsesquioxanes (POSS), POSS nanocomposites and their applications: A review. *J. Sci. Ind. Res.* **2009**, *68*, 437–464.
14. Chou, C.H.; Hsu, S.L.; Dinakaran, K.; Chiu, M.Y.; Wei, K.H. Synthesis and Characterization of Luminescent Polyfluorenes Incorporating Side-Chain-Tethered Polyhedral Oligomeric Silsesquioxane Units. *Macromolecules* **2005**, *38*, 745–751. [CrossRef]
15. Ak, M.; Gacal, B.; Kiskan, B.; Yagci, Y.; Toppare, L. Enhancing electrochromic properties of polypyrrole by silsesquioxane nanocages. *Polymer* **2008**, *49*, 2202–2210. [CrossRef]
16. Guenthner, A.J.; Lamison, K.R.; Lubin, L.M.; Haddad, T.S.; Mabry, J.M. Hansen Solubility Parameters for Octahedral Oligomeric Silsesquioxanes. *Ind. Eng. Chem. Res.* **2012**, *51*, 12282–12293. [CrossRef]
17. Zhang, W.; Müller, A.H.E. Synthesis of tadpole-shaped POSS-containing hybrid polymers via "click chemistry". *Polymer* **2010**, *51*, 2133–2139. [CrossRef]
18. Guo, H.; Meador, M.A.B.; McCorkle, L.; Quade, D.J.; Guo, J.; Hamilton, B.; Cakmak, M. Tailoring Properties of Cross-Linked Polyimide Aerogels for Better Moisture Resistance, Flexibility, and Strength. *ACS Appl. Mater. Interface* **2012**, *4*, 5422–5429. [CrossRef]
19. Maji, K.; Halder, D. POSS-Appended Diphenylalanine: Self-Cleaning, Pollution-Protective, and Fire-Retardant Hybrid Molecular Material. *ACS Omega* **2017**, *2*, 1938–1946. [CrossRef]
20. Pramudya, I.; Rico, C.G.; Lee, C.; Chung, H. POSS-Containing Bioinspired Adhesives with Enhanced Mechanical and Optical Properties for Biomedical Applications. *Biomacromolecules* **2016**, *17*, 3853–3861. [CrossRef]
21. Ueda, K.; Tanaka, K.; Chujo, Y. Fluoroalkyl POSS with Dual Functional Groups as a Molecular Filler for Lowering Refractive Indices and Improving Thermomechanical Properties of PMMA. *Polymers* **2018**, *10*, 1332. [CrossRef]
22. Liu, Y.; Wu, X.; Sun, Y.; Xie, W. POSS Dental Nanocomposite Resin: Synthesis, Shrinkage, Double Bond Conversion, Hardness, and Resistance Properties. *Polymers* **2018**, *10*, 369. [CrossRef]

23. Blanco, I. The Rediscovery of POSS: A Molecule Rather than a Filler. *Polymers* **2018**, *10*, 904. [CrossRef]
24. Huang, K.W.; Tsai, L.W.; Kuo, S.W. Influence of octakis-functionalized polyhedral oligomeric silsesquioxanes on the physical properties of their polymer nanocomposites. *Polymer* **2009**, *50*, 4876–4887. [CrossRef]
25. Blanco, I.; Abate, L.; Bottino, F.A. Mono substituted octaphenyl POSSs: The effects of substituents on thermal properties and solubility. *Thermochim. Acta* **2017**, *655*, 117–123. [CrossRef]
26. Blanco, I.; Bottino, F.A. The influence of the nature of POSSs cage's periphery on the thermal stability of a series of new bridged POSS/PS nanocomposites. *Polym. Degrad. Stab.* **2015**, *121*, 180–186. [CrossRef]
27. Hu, W.H.; Huang, K.W.; Chiou, C.W.; Kuo, S.W. Complementary Multiple Hydrogen Bonding Interactions Induce the Self-Assembly of Supramolecular Structures from Heteronucleobase-Functionalized Benzoxazine and Polyhedral Oligomeric Silsesquioxane Nanoparticles. *Macromolecules* **2012**, *45*, 9020–9028. [CrossRef]
28. Wu, Y.C.; Kuo, S.W. Self-assembly supramolecular structure through complementary multiple hydrogen bonding of heteronucleobase-multifunctionalized polyhedral oligomeric silsesquioxane (POSS) complexes. *J. Mater. Chem.* **2012**, *22*, 2982–2991. [CrossRef]
29. Chiou, C.W.; Lin, Y.C.; Wang, L.; Hirano, C.; Suzuki, Y.; Hayakawa, T.; Kuo, S.W. Strong Screening Effect of Polyhedral Oligomeric Silsesquioxanes (POSS) Nanoparticles on Hydrogen Bonded Polymer Blends. *Polymers* **2014**, *6*, 926–948. [CrossRef]
30. Chen, W.C.; Lin, R.C.; Tseng, S.M.; Kuo, S.W. Minimizing the Strong Screening Effect of Polyhedral Oligomeric Silsesquioxane Nanoparticles in Hydrogen-Bonded Random Copolymers. *Polymers* **2018**, *10*, 303. [CrossRef]
31. Mohamed, M.G.; Kuo, S.W. Polybenzoxazine/Polyhedral Oligomeric Silsesquioxane (POSS) Nanocomposites. *Polymers* **2016**, *6*, 225. [CrossRef]
32. Mohamed, M.G.; Hsu, K.C.; Hong, J.L.; Kuo, S.W. Unexpected fluorescence from maleimide-containing polyhedral oligomeric silsesquioxanes: Nanoparticle and sequence distribution analyses of polystyrene-based alternating copolymers. *Polym. Chem.* **2016**, *7*, 135–145. [CrossRef]
33. Laine, R.M.; Roll, M.F. Polyhedral Phenylsilsesquioxanes. *Macromolecules* **2011**, *44*, 1073–1109. [CrossRef]
34. Lin, Y.C.; Kuo, S.W. Hierarchical self-assembly structures of POSS-containing polypeptide block copolymers synthesized using a combination of ATRP, ROP and click chemistry. *Polym. Chem.* **2012**, *3*, 882–891. [CrossRef]
35. Lin, Y.C.; Kuo, S.W. Hierarchical self-assembly and secondary structures of linear polypeptides graft onto POSS in the side chain through click chemistry. *Polym. Chem.* **2012**, *3*, 162–171. [CrossRef]
36. Tomasz, P.; Anna, K.; Bozena, Z.; Marek, J.P. Structure, dynamics, and host-guest interactions in POSS functionalized cross-linked nanoporous hybrid organic-inorganic polymers. *J. Phys. Chem. C* **2015**, *119*, 26575–26587.
37. Liao, Y.T.; Lin, Y.C.; Kuo, S.W. Highly Thermally Stable, Transparent, and Flexible Polybenzoxazine Nanocomposites by Combination of Double-Decker-Shaped Polyhedral Silsesquioxanes and Polydimethylsiloxane. *Macromolecules* **2017**, *50*, 5739–5747. [CrossRef]
38. Hong, B.; Thoms, T.P.S.; Murfee, H.J.; Lebrun, M.L. Highly dendritic macromolecules with core polyhedral silsesquioxane functionalities. *Inorg. Chem.* **1997**, *36*, 6146–6147. [CrossRef]
39. Phillips, S.H.; Haddad, T.S.; Tomczak, S.J. Development in nanoscience: Polyherdral oligomeric silsesquioxane (POSS)-polymers. *Curr. Opin. Solid State Mater. Sci.* **2004**, *8*, 21–29. [CrossRef]
40. Ayandele, E.; Sarkar, B.; Alexandridis, P. Polyhedral Oligomeric Silsesquioxane (POSS)-Containing Polymer Nanocomposites. *Nanomaterials* **2012**, *2*, 445–475. [CrossRef]
41. Balazs, A.C.; Emrick, T.; Russell, T.P. Nanoparticle polymer composites: Where two small worlds meet. *Science* **2006**, *314*, 1107–1110. [CrossRef] [PubMed]
42. Anderson, J.A.; Sknepnek, R.; Travesset, A. Design of polymer nanocomposites in solution by polymer functionalization. *Phys. Rev. E* **2010**, *82*, 021803–0218011. [CrossRef] [PubMed]
43. Bockstaller, M.R.; Mickiewicz, R.A.; Thomas, E.L. Block copolymer nanocomposites: Perspectives for tailored functional materials. *Adv. Mater.* **2005**, *17*, 1331–1349. [CrossRef]
44. Ahmad, Z.; Mark, J.E. Polyimide-Ceramic Hybrid Composites by the Sol-Gel Route. *Chem. Mater.* **2001**, *13*, 3320–3330. [CrossRef]
45. Govindaraj, B.; Sundararajanb, P.; Muthusamy Sarojadevi, M. Synthesis and characterization of polyimide/polyhedral oligomeric silsesquioxane nanocomposites containing quinolyl moiety. *Polym. Int.* **2012**, *61*, 1344–1352. [CrossRef]

46. Ando, S.; Harada, M.; Okada, T.; Ishige, R. Effective Reduction of Volumetric Thermal Expansion of Aromatic Polyimide Films by Incorporating Interchain Crosslinking. *Polymers* **2018**, *10*, 761. [CrossRef]
47. Mathews, A.S.; Kim, I.; Ha, C.S. Fully aliphatic polyimides from adamantane-based diamines for enhanced thermal stability, solubility, transparency, and low dielectric constant. *J. Appl. Polym. Sci.* **2006**, *102*, 3316–3326. [CrossRef]
48. Liaw, D.-J.; Liaw, B.-Y.; Li, L.-J.; Sillion, B.; Mercier, R.; Thiria, R.; Sekiguchi, H. Synthesis and characterization of new soluble polyimides from 3,3′,4,4′-benzhydrol tetracarboxylic dianhydride and various diamines. *Chem. Mater.* **1998**, *10*, 734–739. [CrossRef]
49. Wachsman, E.D.; Frank, C.W. Effect of cure history on the morphology of polyimide: Fluorescence spectroscopy as a method for determining the degree of cure. *Polymer* **1988**, *29*, 1191–1197. [CrossRef]
50. Sroog, C.E. Polyimides. *J. Polym. Sci. Macromol. Rev.* **1976**, *11*, 161–208. [CrossRef]
51. Choi, J.Y.; Yu, H.C.; Lee, J.; Jeon, J.; Im, J.; Jan, J.; Jin, S.W.; Kim, K.K.; Cho, S.; Chung, C.M. Preparation of Polyimide/Graphene Oxide Nanocomposite and Its Application to Nonvolatile Resistive Memory Device. *Polymers* **2018**, *10*, 901. [CrossRef]
52. Chen, Y.; Lin, B.; Zhang, X.; Wang, J.; Lai, C.; Sun, Y.; Liu, Y.; Yang, H. Enhanced Dielectric Properties of Amino-Modified-CNT/Polyimide Composite Films with A Sandwich Structure. *J. Mater. Chem. A* **2014**, *2*, 14118–14126. [CrossRef]
53. Lei, X.; Chen, Y.; Qiao, M.; Tian, L.; Zhang, Q. Hyperbranched Polysiloxane (HBPSi)-Based Polyimide Films with Ultralow Dielectric Permittivity, Desirable Mechanical and Thermal Properties. *J. Mater. Chem. C* **2016**, *14*, 2134–2146. [CrossRef]
54. Simpson, J.O.; St. Clair, A.K. Fundamental Insight on Developing Low Dielectric Constant Polyimides. *Thin Solid Films* **1997**, *309*, 480–485. [CrossRef]
55. Lyulin, S.V.; Larin, S.V.; Gurtovenko, A.A.; Nazarychev, V.M.; Falkovich, S.G.; Yudin, V.E.; Svetlichnyi, V.M.; Gofman, I.V.; Lyulin, A.V. Thermal Properties of Bulk Polyimides: Insights from Computer Modeling Versus Experiment. *Soft Matter* **2014**, *10*, 1224–1232. [CrossRef] [PubMed]
56. Chi, Q.; Sun, J.; Zhang, C.; Liu, G.; Lin, J.; Wang, Y.; Wang, X.; Lei, Q. Enhanced Dielectric Performance of Amorphous Calcium Copper Titanate/Polyimide Hybrid Film. *J. Mater. Chem. C* **2014**, *2*, 172–177. [CrossRef]
57. Liao, W.H.; Yang, S.Y.; Hsiao, S.T.; Wang, Y.S.; Li, S.M.; Tien, H.W.; Ma, C.C.M.; Zeng, S.J. A Novel Approach to Prepare Graphene Oxide/Soluble Polyimide Composite Films with A Low Dielectric Constant and High Mechanical Properties. *RSC Adv.* **2014**, *4*, 51117–51125. [CrossRef]
58. Lei, X.F.; Chen, Y.; Zhang, H.P.; Li, X.J.; Yao, P.; Zhang, Q.Y. Space Survivable Polyimides with Excellent Optical Transparency and Self-Healing Properties Derived from Hyperbranched Polysiloxane. *ACS Appl. Mater. Interfaces* **2013**, *5*, 10207–10220. [CrossRef]
59. Kim, S.; Wang, X.; Ando, S.; Wang, X. Low Dielectric and Thermally Stable Hybrid Ternary Composites of Hyperbranched and Linear Polyimides with SiO_2. *RSC Adv.* **2014**, *4*, 27267–27276. [CrossRef]
60. Hasegawa, M.; Horiuchi, M.; Wada, Y. Polyimides Containing Trans-1,4-cyclohexane Unit (II). Low-K and Low-CTE Semi- and Wholly Cycloaliphatic Polyimides. *High Perform. Polym.* **2007**, *19*, 175–193. [CrossRef]
61. Fan, H.; Yang, R. Flame-Retardant Polyimide Cross-Linked with Polyhedral Oligomeric Octa(aminophenyl)silsesquioxane. *Ind. Eng. Chem. Res.* **2013**, *52*, 2493–2500. [CrossRef]
62. Zhang, L.; Tian, G.; Wang, X.; Qi, S.; Wu, Z.; Wu, D. Polyimide/ladder-like polysilsesquioxane hybrid films: Mechanical performance, microstructure and phase separation behaviors. *Compos. Part B* **2014**, *56*, 808–810. [CrossRef]
63. Wu, Y.W.; Zhang, W.C.; Yang, R.J. Ultralight and Low Thermal Conductivity Polyimide-Polyhedral Oligomeric Silsesquioxanes Aerogels. *Macromol. Mater. Eng.* **2017**, 1700403–1700415. [CrossRef]
64. Tyan, H.L.; Leu, C.M.; Wei, K.H. Effect of Reactivity of Organics-Modified Montmorillonite on the Thermal and Mechanical Properties of Montmorillonite/Polyimide Nanocomposites. *Chem. Mater.* **2001**, *13*, 222–226. [CrossRef]
65. Wu, S.; Hayakawa, T.; Kakimoto, M.; Oikawa, H. Synthesis and Characterization of Organosoluble Aromatic Polyimides Containing POSS in Main Chain Derived from Double-Decker-Shaped Silsesquioxane. *Macromolecules* **2008**, *41*, 3481–3487. [CrossRef]
66. Jiang, L.Y.; Wei, K.H. Bulk and surface properties of layered silicates/fluorinated polyimide nanocomposites. *J. Appl. Phys.* **2002**, *92*, 6219–6223. [CrossRef]

67. Huang, J.; He, C.; Xiao, Y.; Mya, K.Y.; Dai, J.; Siow, Y.P. Polyimide/POSS nanocomposites: Interfacial interaction, thermal properties and mechanical properties. *Polymer* **2003**, *44*, 4491–4499. [CrossRef]
68. Tamaki, R.; Choi, J.; Laine, R.A. Polyimide Nanocomposite from Octa(aminophenyl)silsesquioxane. *Chem. Mater.* **2003**, *15*, 793–797. [CrossRef]
69. Lin, C.H.; Chang, S.L.; Cheng, P.W. Soluble high-T_g polyetherimides with good flame retardancy based on an asymmetric phosphinated etherdiamine. *J. Polym. Sci. Part A Polym. Chem.* **2011**, *49*, 1331–1340. [CrossRef]
70. Ye, Y.S.; Chen, W.Y.; Wang, Y.Z. Synthesis and Properties of Low-Dielectric-Constant Polyimides with Introduced Reactive Fluorine Polyhedral Oligomeric Silsesquioxanes. *J. Polym. Sci. Part A Polym.* **2006**, *44*, 5391–5402. [CrossRef]
71. Ye, Y.S.; Yen, Y.C.; Chen, W.Y.; Cheng, C.C.; Chang, F.C. A simple approach toward low-dielectric polyimide nanocomposites: Blending the polyimide precursor with a fluorinated polyhedral oligomeric silsesquioxane. *J. Polym. Sci. Part A Polym. Chem.* **2008**, *46*, 6292–6304. [CrossRef]
72. Liu, H.; Zheng, S.; Nie, K. Morphology and Thermomechanical Properties of Organic-Inorganic Hybrid Composites Involving Epoxy Resin and an Incompletely Condensed Polyhedral Oligomeric Silsesquioxane. *Macromolecules* **2005**, *38*, 5088–5097. [CrossRef]
73. Xu, H.; Kuo, S.W.; Lee, J.S.; Chang, F.C. Glass transition temperatures of poly(hydroxystyrene-co-vinylpyrrolidone-co-isobutylstyrylpolyhedraloligosilsesquioxanes). *Polymer* **2003**, *43*, 5117–5124. [CrossRef]
74. Liao, W.H.; Yang, Y.S.; Hsiao, T.S.; Wang, Y.S.; Li, M.S.; Ma, C.C.; Tien, H.W.; Zeng, J.S. Effect of Octa(aminophenyl) Polyhedral Oligomeric Silsesquioxane Functionalized Graphene Oxide on the Mechanical and Dielectric Properties of Polyimide Composites. *ACS Appl. Mater. Interfaces* **2014**, *6*, 15802–15812. [CrossRef] [PubMed]
75. Lee, Y.J.; Huang, J.M.; Kuo, S.W.; Chang, F.C. Low-dielectric, nanoporous polyimide films prepared from PEO-POSS NPs. *Polymer* **2005**, *46*, 10056–10065. [CrossRef]
76. Leu, C.M.; Reddy, G.M.; Wei, K.H.; Shu, C.F. Synthesis and Dielectric Properties of Polyimide-Chain-End Tethered Polyhedral Oligomeric Silsesquioxane Nanocomposites. *Chem. Mater.* **2003**, *15*, 2261–2265. [CrossRef]
77. Wang, C.Y.; Chen, W.T.; Xu, C.; Zhao, X.Y.; Jian, L. Fluorinated Polyimide/POSS Hybrid Polymers with High Solubility and Low Dielectric Constant. *Chin. J. Polym. Sci.* **2016**, *34*, 1363–1372. [CrossRef]
78. Leu, C.M.; Chang, Y.T.; Wei, K.H. Synthesis and Dielectric Properties of Polyimide-Tethered Polyhedral Oligomeric Silsesquioxane (POSS) Nanocomposites via POSS-diamine. *Macromolecules* **2003**, *36*, 9122–9127. [CrossRef]
79. Chen, Y.; Chen, L.; Nie, H.; Kang, E.T. Low-k Nanocomposite Films Based on Polyimides with Grafted Polyhedral Oligomeric Silsesquioxane. *J. Appl. Polym. Sci.* **2006**, *99*, 2226–2232. [CrossRef]
80. Wu, S.; Hayakawa, T.; Kikuchi, R.; Grunzinger, S.J.; Kakimoto, M. Synthesis and Characterization of Semiaromatic Polyimides Containing POSS in Main Chain Derived from Double-Decker-Shaped Silsesquioxane. *Macromolecules* **2007**, *40*, 5698–5705. [CrossRef]
81. Qiu, J.; Xu, S.; Liu, N.; Wei, K.; Li, L.; Zheng, S. Organic–inorganic polyimide nanocomposites containing a tetrafunctional polyhedral oligomeric silsesquioxane amine: Synthesis, morphology and thermomechanical properties. *Polym. Int.* **2018**, *67*, 301–312. [CrossRef]
82. Zheng, S.; Wang, L.; Liu, N. Organic-inorganic polyimides with double decker silsesquioxane in the main chains. *Polym. Chem.* **2016**, *7*, 1158–1167.
83. Lee, Y.J.; Huang, J.M.; Kuo, S.W.; Lu, J.S.; Chang, F.C. Polyimide and polyhedral oligomeric silsesquioxane nanocomposites for low-dielectric applications. *Polymer* **2005**, *46*, 173–181. [CrossRef]
84. Gong, C.; Liang, Y.; Qi, Z.; Li, H.; Wu, Z.; Zhang, Z.; Zhang, S.; Zhang, X.; Li, Y. Solution processable octa(aminophenyl)silsesquioxane covalently cross-linked sulfonated polyimides for proton exchange membranes. *J. Membr. Sci.* **2015**, *476*, 364–372. [CrossRef]

85. Devaraju, S.; Vengatesan, M.R.; Selvi, M.; Kumar, A.A.; Alagar, M. Synthesis and characterization of bisphenol-A ether diamine-based polyimide POSS nanocomposites for low K dielectric and flame-retardant applications. *High Perform. Polym.* **2012**, *24*, 85–96. [CrossRef]
86. Seckin, T.; Köytepe, S.; Adıgüzel, H.I. Molecular design of POSS core star polyimides as a route to low-k dielectric materials. *Mater. Chem. Phys.* **2008**, *112*, 1040–1046. [CrossRef]